Research in Astronomy and Astrophysics, 24:125021 (7pp), 2024 December https://doi.org/10.1088/1674-4527/ad9654

Measuring the Time Variation of the Fine-structure Constant with Quasars Detected by LAMOST

Jin-Nan Wei (魏晋南)[1,2,3], Rui-Jie Chen (陈睿劼)[1,4], Jun-Jie Wei (魏俊杰)[1,2], Martín López-Corredoira[5,6,7], and Xue-Feng Wu (吴雪峰)[1,2]

[1] Purple Mountain Observatory, Chinese Academy of Sciences, Nanjing 210023, China; jjwei@pmo.ac.cn, xfwu@pmo.ac.cn
[2] School of Astronomy and Space Sciences, University of Science and Technology of China, Hefei 230026, China
[3] Shanghai Astronomy Museum (branch of Shanghai Science & Technology Museum), Shanghai 201306, China
[4] Department of Physics, Imperial College London, London SW7 2AZ, UK
[5] Instituto de Astrofísica de Canarias, E-38205 La Laguna, Tenerife, Spain
[6] PIFI-Visiting Scientist 2023 of China Academy of Sciences at Purple Mountain Observatory, Nanjing 210023 and National Astronomical Observatories, Beijing 100101, China
[7] Departamento de Astrofísica, Universidad de La Laguna, E-38206 La Laguna, Tenerife, Spain
Received 2024 September 02; revised 2024 November 06; accepted 2024 November 22; published 2024 December 13

Abstract

The [O III] $\lambda\lambda$4960, 5008 emission lines in the optical spectra of galaxies and quasars have been widely used to investigate the possible variation of the fine-structure constant α over cosmic time. In this work, we utilize the Large Sky Area Multi-object Fiber Spectroscopic Telescope (LAMOST) quasar survey, for the first time, to measure the relative α variation $\Delta\alpha/\alpha$ in time through the [O III] doublet method. From the LAMOST Data Release 9 quasar catalog, we refine a sample of 209 quasar spectra with strong and narrow [O III] emission lines over a redshift range of $0 < z < 0.8$. Analysis on all of the 209 spectra obtains $\Delta\alpha/\alpha = (0.5 \pm 3.7) \times 10^{-4}$, which suggests that there is no evidence of varying α on the explored cosmological timescales. Assuming a linear variation, the mean rate of change in $\Delta\alpha/\alpha$ is limited to be $(-3.4 \pm 2.4) \times 10^{-13}\,\mathrm{yr}^{-1}$ in the last 7.0 Gyr. While our LAMOST-based constraint on $\Delta\alpha/\alpha$ is not competitive with those of the Sloan Digital Sky Survey (SDSS) quasar observations, our analysis serves to corroborate the results of SDSS with another independent survey.

Key words: atomic data – (galaxies:) quasars: emission lines – surveys – cosmology: observations

1. Introduction

Fundamental physical constants are assumed to be universal and constant under the current Standard Model of particle physics. However, some modern theories beyond the Standard Model predict that the fundamental constants of nature may vary across space in time (Martins 2017). In the last few decades, many efforts have been devoted to searching for possible variations of these constants, either through laboratory experiments or astrophysical observations (see Uzan 2003, 2011 for a review).

One of the particularly interesting fundamental constants is the fine-structure constant α, defined by $\alpha \equiv e^2/(4\pi\epsilon_0\hbar c)$, where e, ϵ_0, $\hbar$, and c are the electron charge, the permittivity of free space, reduced Planck constant, and speed of light in vacuum, respectively. It is a dimensionless physical constant that characterizes the strength of the electromagnetic force between electrically charged particles. Any possible variations in α could indicate that the laws of physics are not the same everywhere in the Universe or have changed over time. This challenges the assumption of the constancy of physical laws, which is a cornerstone of modern physics. Moreover, variations in α could imply the existence of new physics beyond the Standard Model, such as extra dimensions or varying scalar fields. This would have profound implications for our understanding of the Universe. By studying potential variations in α, physicists and astronomers can examine the robustness of the fundamental laws of nature, test alternative cosmological models that account for varying α (Martins & Pinho 2015; Martins et al. 2015), and potentially uncover new aspects of the Universe's underlying structure (Mota & Barrow 2004).

The fundamental constant α also quantifies the separation in the fine-structure of atomic spectral lines (e.g., Dzuba et al. 1999a; Uzan 2003). Any relative α variation (i.e., $\Delta\alpha/\alpha$) over time can therefore be measured directly by comparing the wavelengths of fine-structure splitting of atomic lines at two different epochs. Astrophysical spectra involving long look-back times have been widely used to investigate the possible variation of α. The first measurements on the α variation from astronomical spectroscopy reached an accuracy of $\Delta\alpha/\alpha \approx 10^{-2}$–$10^{-3}$ (Savedoff 1956; Bahcall & Salpeter 1965; Bahcall & Schmidt 1967; Bahcall et al. 1967). Since then, the methodologies for analyzing spectra and our understanding of systematic errors have improved significantly. At present, there are two main methods to measure the relative separation of

absorption lines in the spectra of quasars, i.e., the alkali-doublet (AD) method (Bahcall et al. 1967) and the many-multiplet (MM) method (Dzuba et al. 1999b; Webb et al. 1999).

In the AD method, the adopted quasar absorption lines were mainly fine-structure doublet lines, such as C IV, N V, Mg II, and Si IV (e.g., Potekhin & Varshalovich 1994; Cowie & Songaila 1995; Murphy et al. 2001b; Chand et al. 2005). The current best constraints obtained using the AD method are those based on the analysis of Si IV absorption lines, yielding $\Delta\alpha/\alpha = (1.5 \pm 4.3) \times 10^{-6}$ over a redshift range of $1.59 \leqslant z \leqslant 2.92$ (Chand et al. 2005). The MM method simultaneously analyzes all (or most) doublets of many atomic species, thereby achieving a higher precision compared to the AD method. Using the MM method, some early works claimed to have found tentative evidence for variation of α at a level of $\Delta\alpha/\alpha \sim$ (1–10) $\times 10^{-6}$ (e.g., Murphy et al. 2001a, 2003; Webb et al. 2001, 2011). However, subsequent works indicated that such variations were likely to be caused by wavelength distortions and other systematic effects (e.g., Evans et al. 2014; Whitmore & Murphy 2015). Recently, Murphy et al. (2022) applied the MM method to the absorption spectra of nearby star twins within 50 pc, and found no variations in α with a precision of 5.0×10^{-8}. Although more precise, the MM method still suffers from a number of uncertainties (see Webb et al. 2022 for a recent review), which may arise from the techniques for correcting wavelength distortion (Dumont & Webb 2017), the assumptions underlying the Voigt fitting technique (Levshakov 2004), the technical details of profile fitting (Bainbridge & Webb 2017; Lee et al. 2023), the unconsidered systematic errors (Lee et al. 2021), and other. These uncertainties may induce biases on the values of $\Delta\alpha/\alpha$ and underestimations of their errors. Thus, different methods are encouraged to cross-check the results of the MM method.

In this work, we employ the method based on the [O III] emission lines, first proposed by Bahcall & Salpeter (1965), to constrain possible variations in α. Since the [O III] doublet method relies only on a pair of lines, the limits on $\Delta\alpha/\alpha$ are not as stringent as those obtained with the MM method but have the advantage of being more transparent and less subject to systematics. The [O III] $\lambda\lambda$4960, 5008 doublet lines originate in the downward transitions from the same upper energy level of the same ion, so no assumptions on ionization state, chemical composition, or distribution of energy levels are required in practice. The [O III] doublet method therefore represents an excellent alternative for measuring the α variation on a firm basis. The $\Delta\alpha/\alpha$ constraints obtained by recent works based on the [O III] emission lines are summarized as follows. By analyzing 42 quasar spectra from the Early Data Release of Sloan Digital Sky Survey (SDSS), Bahcall et al. (2004) derived $\Delta\alpha/\alpha = (0.7 \pm 1.4) \times 10^{-4}$ over the range $0.16 < z < 0.8$. Gutiérrez & López-Corredoira (2010) obtained $\Delta\alpha/\alpha = (2.4 \pm 2.5) \times 10^{-5}$ using 1568 quasar spectra at $0.0 < z < 0.8$ from SDSS Data Release 6 (DR6). Rahmani et al. (2014) derived $\Delta\alpha/\alpha = (-2.1 \pm 1.6) \times 10^{-5}$ using 2347 quasar spectra at $0.02 < z < 0.74$ from SDSS DR7. Albareti et al. (2015) obtained $\Delta\alpha/\alpha = (0.9 \pm 1.8) \times 10^{-5}$ using 13,175 quasar spectra at $0.04 < z < 1.0$ from SDSS DR12. Li et al. (2024) analyzed 40 spectra of Lyα emitting galaxies and 46 spectra of quasars at $1.09 < z < 3.73$ using the VLT/X-Shooter spectra publicly available, from which they yielded $\Delta\alpha/\alpha = (-3 \pm 6) \times 10^{-5}$. Jiang et al. (2024a) measured $\Delta\alpha/\alpha = (2 \sim 3) \times 10^{-5}$ by utilizing ~110,000 [O III] emission-line galaxies at $0 < z < 0.95$ from the Dark Energy Spectroscopic Instrument. Jiang et al. (2024b) obtained $\Delta\alpha/\alpha = (0.4 \pm 0.7) \times 10^{-4}$ using 572 JWST spectra from 522 [O III] emission-line galaxies at $3 < z < 10$. In addition to the [O III] emission lines, other emission doublets, such as [Ne III] $\lambda\lambda$3869, 3968 and [S II] $\lambda\lambda$6717, 6731, have also been used to explore the α variation (e.g., Gutiérrez & López-Corredoira 2010; Albareti et al. 2015). However, the limits of their accuracy are worse, because all these doublets in quasars are fainter than [O III] and some of them are affected by systematic errors.

Recently, the Large Sky Area Multi-object Fiber Spectroscopic Telescope (LAMOST) released the results of its 9 yr quasar survey (Jin et al. 2023). Here, we use the latest LAMOST DR9 quasar sample, for the first time, to measure the time variation of α through the [O III] doublet method. Our analysis can serve to corroborate previous results of SDSS with another independent survey, thereby discarding possible systematic errors in the wavelength calibration of quasar spectra in SDSS. The rest of this paper is organized as follows. In Section 2, we introduce our quasar sample and spectroscopic data. Our resulting constraints on $\Delta\alpha/\alpha$ are then presented in Section 3. Finally, a brief summary and discussions are drawn in Section 4.

2. LAMOST Data and Wavelength Measurements

In this section, we will first clarify why the [O III] doublet can provide an ideal testbed for measuring the α variation. We will then describe the LAMOST quasar survey and the refined sample used for our analysis. Finally, we will introduce the measurements of emission-line wavelengths in detail.

2.1. [O III] Doublet as a Testbed for Varying α

The variation in the fine-structure constant α can be measured through the wavelength separation of absorption or emission multiplets in the quasar spectra as (Uzan 2003)

$$\frac{\Delta\alpha}{\alpha}(z) = \frac{1}{2}\left\{\frac{[(\lambda_2 - \lambda_1)/(\lambda_2 + \lambda_1)]_z}{[(\lambda_2 - \lambda_1)/(\lambda_2 + \lambda_1)]_0} - 1\right\}, \quad (1)$$

where λ_1 and λ_2 are the shorter and longer wavelengths of the pairs of the doublet, and the subscripts 0 and z stand for the wavelength values at redshift zero (laboratory values) and at redshift z, respectively.

The present-day vacuum wavelengths of the [O III] doublet lines are $\lambda_1(0) = 4960.295$ Å and $\lambda_2(0) = 5008.240$ Å, respectively.[8] Concerning emission lines, the [O III] doublet is the most suitable pair of lines for measuring $\Delta\alpha/\alpha$. The reasons are as follows. First, the doublet lines have a wide wavelength separation, $\Delta\lambda_0 = [\lambda_2 - \lambda_1]_0 = 47.945$ Å, representing almost one order of magnitude wider than most of the fine-structure doublets. Note that the sensitivity of $\Delta\alpha/\alpha$ is positively related to the wavelength separation. For illustrative purposes, Equation (1) can be approximated as $\Delta\alpha/\alpha \approx 0.5 \times \epsilon/\Delta\lambda_0$, where $\epsilon = \Delta\lambda_z/(1+z) - \Delta\lambda_0$ denotes the difference between the measured wavelength separation at redshift z in rest frame and the local one. It is obvious from this formula that a difference of $\epsilon = 0.01$ Å for [O III] implies $\Delta\alpha/\alpha \approx 10^{-4}$. That is, a statistical or systematic uncertainty of 0.01 Å places a measuring precision of $\Delta\alpha/\alpha \approx 10^{-4}$. Second, the [O III] doublet often appears in quasar spectra with relatively high signal-to-noise ratio (S/N). Compared to other doublets, it is easier to extract the wavelength values of the [O III] lines, which is crucial for the $\Delta\alpha/\alpha$ constraint.

2.2. LAMOST Quasar Survey and Sample Selection

LAMOST, also called the Guoshoujing Telescope, is a special quasi-meridian reflecting Schmidt telescope located at Xinglong Observatory, China (Wang et al. 1996; Su & Cui 2004; Cui et al. 2012; Zhao et al. 2012). The available large focal surface is circular with a diameter of 1.75 m (~5° field of view), 4000 fibers are almost uniformly distributed over it. Each spectrum obtained by LAMOST is divided into two channels (blue and red) whose wavelength coverage is 3700–5900 Å and 5700–9000 Å, respectively, with an overlapping region at 5700–5900 Å. The spectra have a resolution of $R \sim 1000$–2000 over the entire wavelength range.

After the two year commissioning period, a pilot spectroscopic survey with LAMOST was conducted between 2011 October and 2012 June (Luo et al. 2012). The LAMOST regular survey officially begins in 2012 September, which consists of two main tasks (Zhao et al. 2012): the LAMOST Experiment for Galactic Understanding and Exploration survey (LEGUE), and the LAMOST ExtraGAlactic Survey (LEGAS). The LAMOST quasar survey is affiliated with LEGAS. Despite only a small portion of the observation time being used to search for quasars due to the limitations of the observation site (e.g., bad weather, poor seeing, and bright background), a total of 56,175 quasars have already been identified by LAMOST, 24,127 of which were newly discovered, during the first 9 yr quasar survey (Jin et al. 2023).

In this work, we make use of the LAMOST low resolution catalog of emission-line features of quasars to investigate the possible variation of α over cosmic time. All the quasar spectra used for our analysis are downloaded from LAMOST's official website.[9] In order to effectively refine the final sample from the LAMOST DR9 catalog, our sample selection criteria include the following aspects.

(i) Those quasars with redshifts $\leqslant 0.8$ are selected. This restriction is imposed by the wavelength range of the LAMOST spectrograph (3700–9000 Å) and the wavelength positions of the [O III] $\lambda\lambda$4960, 5008 doublet lines. This criterion removes the sample down to 16,902 quasars.

(ii) Those targets with strong [O III] emission lines are selected. Since the λ4960 line is always weaker than the λ5008 line, the selection of the final sample is determined mainly on the basis of the strength of the λ4960 line. We require the peak flux density of the weaker [O III] line (4960 Å) to be larger than 10^{-19} erg s^{-1} cm^{-2} Å^{-1} and its $S/N_{[O\ III]\ 4960}$ to be above 3. This criterion significantly reduces the sample from 16,902 to 373 objects.

(iii) Those targets with high goodness-of-fit are selected. Owing to the low resolution mode of the LAMOST quasar survey, there are some scenarios in which the Gaussian fits to the spectral lines do not converge. This criterion causes us to further discard 164 spectra. Hence, there are 209 remaining quasar spectra in our final sample.

2.3. Measurements of Emission-line Wavelengths

The emission-line properties of the [O III] doublet can be measured by fitting the LAMOST released spectra. Following Jin et al. (2023), we adopt the publicly available Python code (*PYQSOFIT*; Guo et al. 2018) and its extended package (*QSOFITMORE*; Fu 2021) to fit the spectra. With the estimated uncertainties of the pixels that derived from the reduction pipeline, the *PYQSOFIT* code performs the χ^2 fits. Before the fitting, each quasar spectrum should be corrected for Galactic extinction using the reddening map of Schlegel et al. (1998) with an extinction curve of $R_V = 3.1$ (Fitzpatrick 1999). After the extinction correction, the spectrum is then transformed into the rest frame by using the redshift z.

We estimate the continuum by fitting a broken power law ($f_{\rm bpl}$) and an iron model ($f_{\rm Fe\ II}$) to the rest-frame spectrum, masking those wavelength windows that contain quasar emission lines and the LAMOST spectral overlapping region. Based on the analysis result of the mean composite quasar spectra obtained by Vanden Berk et al. (2001), we fix the inflection point of the broken power law at 4661 Å in rest frame. Many previous studies have found that a sudden slope change occurs at ~5000 Å in the quasar continuum (e.g., Wills et al. 1985; Vanden Berk et al. 2001). There are two possible reasons for the steeper slope at longer wavelengths. One probable reason is the near-infrared inflection caused by hot dust emission (Elvis et al. 1994). Another reason may be

[8] http://physics.nist.gov/PhysRefData/ASD/lines_form.html

[9] https://www.lamost.org/dr9/v2.0/catalog

the contamination from low-redshift host galaxies, which would contribute a larger proportion at longer wavelengths (Serote Roos et al. 1998; Vanden Berk et al. 2001). Besides the broken power law model, the Fe II model $f_{\rm Fe\,II}$ is also an important component of the continuum template, i.e.,

$$f_{\rm Fe\,II} = b_0 F_{\rm Fe\,II}(\lambda,\ b_1,\ b_2), \tag{2}$$

fwhere b_0 is the normalization, b_1 represents the full width at half maximum (FWHM) of Gaussian profile applied to convolve the Fe II template, and b_2 denotes the wavelength shift acted on the Fe II template. A detailed description of the Fe II template can be found in Jin et al. (2023). Most of the quasar continuum can be well described by the broken power law plus an Fe II template, but some spectra have strange shapes in their continuum. This problem may arise from some uncertainties in the spectral response curve, which are occasionally caused by poor relative flux calibrations and unstable efficiencies of some fibers. To overcome this problem, we add an additional three-order polynomial model ($f_{\rm poly}$; Rakshit et al. 2020; Fu et al. 2022). It is thus clear that the pseudocontinuum would be fitted by two (or three) components:

$$f_{\rm cont} = f_{\rm bpl} + f_{\rm Fe\,II} + (f_{\rm poly}). \tag{3}$$

It is worth emphasizing that one should check whether the quasar spectral data are contaminated by the host galaxy, before fitting the continuum. In general, for high-z ($z \gtrsim 0.5$) or high-luminosity ($\log_{10} L_{5100} \gtrsim 44.5$) quasars, the contamination from the host galaxy is negligible. While for those low-z or low-luminosity quasars, the host galaxy contributes an average of $\sim$15% of the observed emissions and produces a $\sim$0.06 dex overestimate of the continuum luminosity at 5100 Å (Shen et al. 2011). The spectral fitting packages *PYQSOFIT* and *QSOFITMORE* would automatically determine whether the quasar spectrum is contaminated by the host galaxy. If true, the decomposition of the host galaxy would be applied to the spectra. The decomposition is based on the host galaxy template developed by Yip et al. (2004a, 2004b). Examples of the fitting results with and without the host galaxy template are presented in Figures 1(a) and (b), respectively. The coordinate, observation ID, and redshift of each quasar are shown on the top of each plot. It is clear that for the quasar with ID number 77208004, the host contribution can lead to overestimate of the strength of the emission lines at longer wavelengths (see the top panel of Figure 1(a)).

After subtracting the fitted continuum component and the host galaxy contamination (if it exists) from the spectrum, the leftover emission-line components can be fitted with Gaussian profiles. The emission lines of Hβ (narrow and broad components) and [O III] $\lambda\lambda$4960, 5008 within the rest-frame window [4640, 5100] Å are simultaneously fitted. The broad component of Hβ is modeled by two Gaussian profiles, and its narrow component is fitted by a single Gaussian. Here we are used to setting the upper limit of FWHM for the narrow components to be 900 km s^{-1}, which is the FWHM criterion for distinguishing between the narrow and broad components (Wang et al. 2009; Coffey et al. 2019; Wang et al. 2019). In principle, the contribution of the broad Hβ emission-line could produce a blueshift in the estimation of the [O III] line positions, particularly affecting the weak 4960 Å line. That is, in addition to a narrow component, the [O III] $\lambda\lambda$4960, 5008 doublet lines should include blue wing components (e.g., Chadid et al. 2004; Schmidt et al. 2018). Therefore, both of the [O III] $\lambda\lambda$4960, 5008 lines are modeled by two Gaussian profiles, one for the line core and the other for the blueshifted wing, and neither of them is correlated with the narrow component of Hβ. The wavelength position of each line of the [O III] doublet can then be directly estimated as the central position of the corresponding Gaussian for the line core. Examples of the best-fitting results of the Hβ–[O III] emission lines are given in the bottom panels of Figures 1(a) and (b). The resulting goodness-of-fit values of reduced χ^2_r are also shown in the figures.

3. Results on the α Variation

We use a total of 209 quasar spectra, drawn from the LAMOST DR9 catalog, after applying the selection criteria (i)–(iii) (see Section 2.2), to measure $\Delta\alpha/\alpha$. With the wavelength measurements of the [O III] $\lambda\lambda$4960, 5008 doublet lines for each quasar spectra, we calculate $\Delta\alpha/\alpha$ using Equation (1). Our results show that most of the $\Delta\alpha/\alpha$ measurements are consistent with 0 within 3σ confidence level, and the accuracies of $\Delta\alpha/\alpha$ are between 10^{-4} and 10^{-2}. Figure 2 shows the rest-frame wavelength measurements of the [O III] doublet lines of all 209 quasar spectra in our final sample. One can see from this plot that the wavelengths of the two lines are aligned along a line from bottom left to top right, showing no systematic effects.

With a series of measured values $x_i = (\Delta\alpha/\alpha)_i$, we calculate the weighted average for the final sample through

$$\bar{x} = \frac{\sum_i x_i/\sigma_i^2}{\sum_i 1/\sigma_i^2}, \tag{4}$$

where σ_i is the error of x_i. The corresponding uncertainty on $\bar{x}$ can be obtained from

$$\sigma_{\bar{x}}^2 = \frac{1}{\sum_i 1/\sigma_i^2}\,. \tag{5}$$

The weighted average for all the 209 spectra is $\Delta\alpha/\alpha = (0.5 \pm 3.7) \times 10^{-4}$. This value is compatible with previous results obtained using other observational samples with the same method (Bahcall et al. 2004; Jiang et al. 2024b).

To explore the possible time variation of $\Delta\alpha/\alpha$, we divide the final sample into eight subsamples with redshifts from low to high, with each subsample containing approximately the same number ($N \simeq 26$) of spectra. For each subsample, we also compute the average value of $\Delta\alpha/\alpha$ and its uncertainty through Equations (4) and (5). The averages of $\Delta\alpha/\alpha$ as a

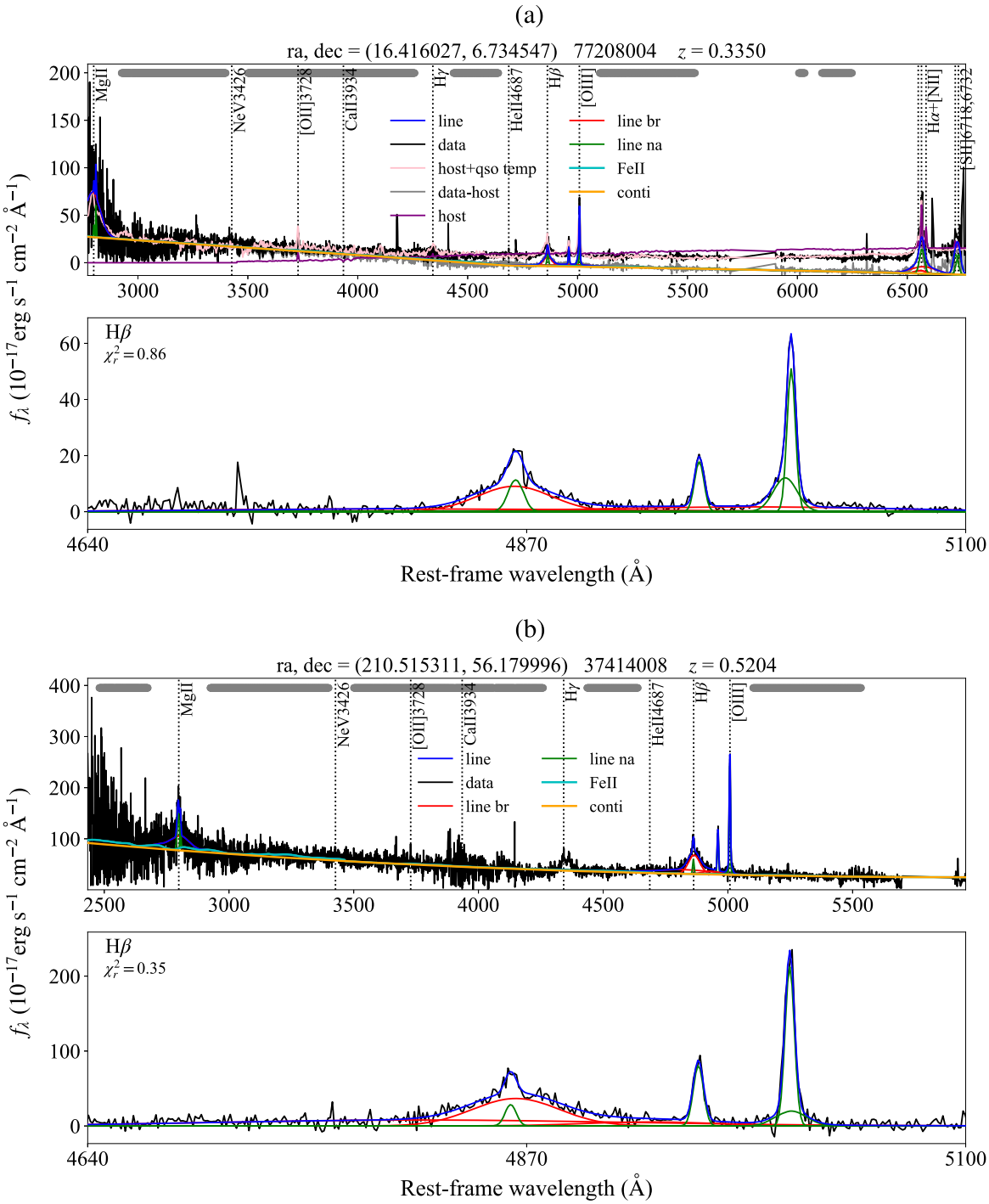

Figure 1. Two examples of the spectral fitting results with (panel (a)) and without (panel (b)) the host galaxy template for quasars whose ID numbers are 77208004 and 37414008. In each pair of panels, the upper panel shows the fitting results of the whole spectrum: the black lines represent the dereddened spectra, the yellow lines denote the continuum model of ($f_{\rm bpl} + f_{\rm poly}$), the cyan lines denote the Fe II template, the purple line represents the host galaxy component, and the gray line represents the dereddened spectrum with the decomposition of the host galaxy. In each pair of panels, the lower panel shows the deblending results of the Hβ–[O III] emission lines: the black lines represent the extinction-corrected spectra with the continuum and the host galaxy contamination (if it exists) subtracted. As for the fitted emission lines, the broad and narrow components are marked in red and green, respectively, and their sums are in blue. The goodness-of-fit χ^2_r are also listed.

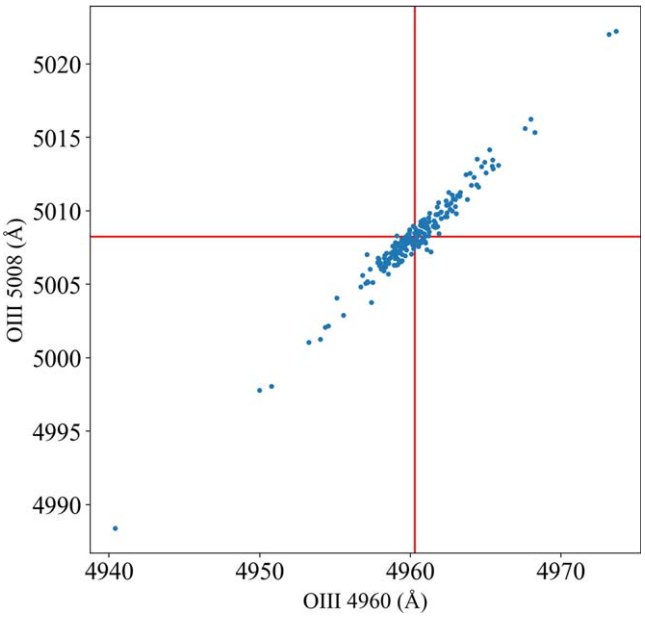

Figure 2. Rest-frame wavelength positions of the two emission lines of the [O III] doublet in our final sample. The vertical and horizontal lines stand for the theoretical local values.

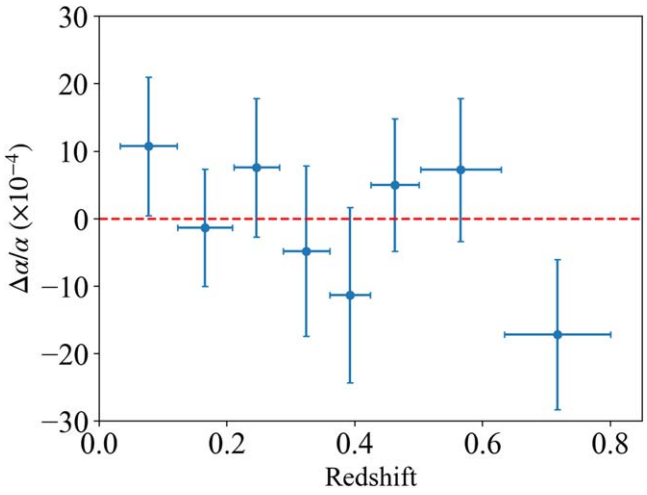

Figure 3. The redshift dependence of the $\Delta\alpha/\alpha$ measurements. Each redshift bin contains the contribution of ∼26 quasar spectra.

function of redshift (or look-back time) are shown in Figure 3 and Table 1. We do not find any variation of $\Delta\alpha/\alpha$ over cosmic time, because none of the $\Delta\alpha/\alpha$ averages deviate from 0 by more than 1.5σ confidence level.

The redshift range of quasars in our final sample is between 0.033 and 0.8, corresponding to a look-back time ($t_{\rm LB}$) of 0.5–7.0 Gyr, or the age of the Universe of 6.8–13.3 Gyr. We assume that α shows linear change with time:

$$\Delta\alpha/\alpha = \kappa \cdot t_{\rm LB} + \omega, \tag{6}$$

where κ and ω are two free parameters. A linear fit of $\Delta\alpha/\alpha$ with respect to $t_{\rm LB}$ for all 209 spectra gives a slope of $\kappa = (-3.4 \pm 2.4) \times 10^{-13}\,{\rm yr}^{-1}$ and an intercept of $\omega = (1.3 \pm 1.0) \times 10^{-3}$. Here the slope $\kappa = d(\Delta\alpha/\alpha)/dt_{\rm LB}$ refers to the mean rate of change in $\Delta\alpha/\alpha$ (Bahcall et al. 2004).

We emphasize that all our results are based on the [O III] emission lines. In principle, by comparing the multiple absorption lines in the damped Lyα systems of quasar spectra, the MM method can achieve higher accuracy than the [O III] doublet method. As the MM method simultaneously analyzes all absorption lines, it requires accurate measurements of both the line wavelengths in the observed spectra and the laboratory wavelengths for all involved atomic transitions. Due to the low resolution of LAMOST, the absorption lines of different atoms are difficult to extract accurately from the observed quasar spectra. Therefore, it is hard to apply the MM method to the quasar sample used here.

Table 1
Average $\Delta\alpha/\alpha$ for Different Redshift Intervals

Redshift Interval	Number	$\Delta\alpha/\alpha$ ($\times10^{-4}$)
0.033–0.122	26	10.8 ± 10.3
0.123–0.208	26	−1.3 ± 8.7
0.211–0.282	26	7.6 ± 10.3
0.288–0.361	26	−4.8 ± 12.7
0.361–0.425	26	−11.3 ± 13.0
0.425–0.500	26	5.0 ± 9.8
0.503–0.629	26	7.3 ± 10.6
0.634–0.801	27	−17.1 ± 11.1

4. Summary and Discussions

In this work, we have used the LAMOST quasar survey, for the first time, to constrain the possible time variation of the fine-structure constant α through the [O III] doublet method. A great advantage of [O III] is that its doublet lines have a wide wavelength separation, which makes it very sensitive to the measurement of the relative α variation $\Delta\alpha/\alpha$. The other advantage is that the [O III] emission lines are much stronger than any other doublets in many quasars, which is crucial for the $\Delta\alpha/\alpha$ measurement.

From 56,175 objects identified as quasars in the LAMOST DR9 quasar catalog, we have extracted a sample of 209 quasars with strong [O III] emission lines up to redshift 0.8. With this refined sample, we estimated a weighted average value of $\Delta\alpha/\alpha = (0.5 \pm 3.7) \times 10^{-4}$ during the last 7.0 Gyr. Due to the smaller number of quasars and the lower resolution of LAMOST with respect to SDSS, our measuring precision of $\Delta\alpha/\alpha$ is worse than previous results obtained using different SDSS quasar samples with the same method by one order of magnitude (Gutiérrez & López-Corredoira 2010; Rahmani et al. 2014;

Albareti et al. 2015). While our LAMOST-based constraint is not competitive, there is merit to the result. Our analysis serves to confirm the results of SDSS with another independent survey, so we can exclude possible systematic errors in the wavelength calibration of spectra in SDSS.

To analyze the value of $\Delta\alpha/\alpha$ as a function of redshift, we divided the sample into eight redshift bins, with each bin containing approximately the same number of quasars. We found that the averages of $\Delta\alpha/\alpha$ in all redshift bins are consistent with 0 within 1.5σ confidence level. This indicates that there is no evidence of changes in $\Delta\alpha/\alpha$ with redshift. We limited the mean rate of change in $\Delta\alpha/\alpha$ to be $(-3.4 \pm 2.4) \times 10^{-13}\,\mathrm{yr}^{-1}$ within the last 7.0 Gyr.

To achieve better constraints on $\Delta\alpha/\alpha$ ($<10^{-6}$) using the emission-line method, high-resolution spectroscopy ($R \sim 100{,}000$) is required. The measurement of $\Delta\alpha/\alpha$ using the LAMOST low resolution spectra is doomed to be unable to reach the best precision from previous quasar observations. Nonetheless, the LAMOST ongoing survey is still collecting useful data, and much more valuable quasars are expected to be identified in the future. The LAMOST quasar survey not only provides an independent measurement of $\Delta\alpha/\alpha$, but also helps to cross-check the results of other surveys. This work only focused on the [O III] doublet, but we will consider more emission lines (e.g., [S II]) in future research. In addition, we plan to discuss collaborative efforts with other observatories to combine data sets, thereby enhancing statistical power for constraining variations in α. For example, there are a total of 56,175 identified quasars in the LAMOST DR9 quasar catalog, of which 24,127 are newly discovered and not reported by SDSS (Jin et al. 2023). We plan to combine the SDSS quasar survey with those new ones discovered by LAMOST to achieve a more robust constraint on $\Delta\alpha/\alpha$.

Acknowledgments

We are grateful to the anonymous referee for the helpful comments. We thank Ye Li for her kind help with the download of the LAMOST data. This work is partially supported by the National Natural Science Foundation of China (grant Nos. 12422307, 12373053, and 12321003), the Key Research Program of Frontier Sciences (grant No. ZDBS-LY-7014) of the Chinese Academy of Sciences, and the Natural Science Foundation of Jiangsu Province (grant No. BK20221562). M.L.C. is supported by the Chinese Academy of Sciences President's International Fellowship Initiative (grant No. 2023VMB0001).

ORCID iDs

Jun-Jie Wei (魏俊杰) https://orcid.org/0000-0003-0162-2488

References

Albareti, F. D., Comparat, J., Gutiérrez, C. M., et al. 2015, MNRAS, 452, 4153
Bahcall, J. N., & Salpeter, E. E. 1965, ApJ, 142, 1677
Bahcall, J. N., Sargent, W. L. W., & Schmidt, M. 1967, ApJL, 149, L11
Bahcall, J. N., & Schmidt, M. 1967, PhRvL, 19, 1294
Bahcall, J. N., Steinhardt, C. L., & Schlegel, D. 2004, ApJ, 600, 520
Bainbridge, M. B., & Webb, J. K. 2017, MNRAS, 468, 1639
Chadid, M., Wade, G. A., Shorlin, S. L. S., & Landstreet, J. D. 2004, A&A, 413, 1087
Chand, H., Petitjean, P., Srianand, R., & Aracil, B. 2005, A&A, 430, 47
Coffey, D., Salvato, M., Merloni, A., et al. 2019, A&A, 625, A123
Cowie, L. L., & Songaila, A. 1995, ApJ, 453, 596
Cui, X.-Q., Zhao, Y.-H., Chu, Y.-Q., et al. 2012, RAA, 12, 1197
Dumont, V., & Webb, J. K. 2017, MNRAS, 468, 1568
Dzuba, V. A., Flambaum, V. V., & Webb, J. K. 1999a, PhRvA, 59, 230
Dzuba, V. A., Flambaum, V. V., & Webb, J. K. 1999b, PhRvL, 82, 888
Elvis, M., Wilkes, B. J., McDowell, J. C., et al. 1994, ApJS, 95, 1
Evans, T. M., Murphy, M. T., Whitmore, J. B., et al. 2014, MNRAS, 445, 128
Fitzpatrick, E. L. 1999, PASP, 111, 63
Fu, Y. 2021, QSOFITMORE: A Python Package for Fitting UV-optical Spectra of Quasars, doi:10.5281/zenodo.5810042
Fu, Y., Wu, X.-B., Jiang, L., et al. 2022, ApJS, 261, 32
Guo, H., Shen, Y., & Wang, S. 2018, PyQSOFit: Python Code to Fit the Spectrum of Quasars, Astrophysics Source Code Library, ascl:1809.008
Gutiérrez, C. M., & López-Corredoira, M. 2010, ApJ, 713, 46
Jiang, L., Pan, Z., Aguilar, J. N., et al. 2024a, ApJ, 968, 120
Jiang, L., Fu, S., Wang, F., et al. 2024b, arXiv:2405.08977
Jin, J.-J., Wu, X.-B., Fu, Y., et al. 2023, ApJS, 265, 25
Lee, C.-C., Webb, J. K., Carswell, R. F., et al. 2023, MNRAS, 521, 850
Lee, C.-C., Webb, J. K., Milaković, D., & Carswell, R. F. 2021, MNRAS, 507, 27
Levshakov, S. A. 2004, in Astrophysics, Clocks and Fundamental Constants, ed. S. G. Karshenboim & E. Peik, Vol. 648 (Berlin: Springer), 151
Li, G., Sun, L., Chen, X., & Zhou, H. 2024, MNRAS, 527, 4913
Luo, A. L., Zhang, H.-T., Zhao, Y.-H., et al. 2012, RAA, 12, 1243
Martins, C. J. A. P. 2017, RPPh, 80, 126902
Martins, C. J. A. P., & Pinho, A. M. M. 2015, PhRvD, 91, 103501
Martins, C. J. A. P., Vielzeuf, P. E., Martinelli, M., Calabrese, E., & Pandolfi, S. 2015, PhLB, 743, 377
Mota, D. F., & Barrow, J. D. 2004, MNRAS, 349, 291
Murphy, M. T., Berke, D. A., Liu, F., et al. 2022, Sci, 378, 634
Murphy, M. T., Webb, J. K., & Flambaum, V. V. 2003, MNRAS, 345, 609
Murphy, M. T., Webb, J. K., Flambaum, V. V., et al. 2001a, MNRAS, 327, 1208
Murphy, M. T., Webb, J. K., Flambaum, V. V., Prochaska, J. X., & Wolfe, A. M. 2001b, MNRAS, 327, 1237
Potekhin, A. Y., & Varshalovich, D. A. 1994, A&AS, 104, 89
Rahmani, H., Maheshwari, N., & Srianand, R. 2014, MNRAS, 439, L70
Rakshit, S., Stalin, C. S., & Kotilainen, J. 2020, ApJS, 249, 17
Savedoff, M. P. 1956, Natur, 178, 688
Schlegel, D. J., Finkbeiner, D. P., & Davis, M. 1998, ApJ, 500, 525
Schmidt, E. O., Oio, G. A., Ferreiro, D., Vega, L., & Weidmann, W. 2018, A&A, 615, A13
Serote Roos, M., Boisson, C., Joly, M., & Ward, M. J. 1998, MNRAS, 301, 1
Shen, Y., Richards, G. T., Strauss, M. A., et al. 2011, ApJS, 194, 45
Su, D.-Q., & Cui, X.-Q. 2004, ChJAA, 4, 1
Uzan, J.-P. 2003, RvMP, 75, 403
Uzan, J.-P. 2011, LRR, 14, 2
Vanden Berk, D. E., Richards, G. T., Bauer, A., et al. 2001, AJ, 122, 549
Wang, J.-G., Dong, X.-B., Wang, T.-G., et al. 2009, ApJ, 707, 1334
Wang, S.-G., Su, D.-Q., Chu, Y.-Q., Cui, X., & Wang, Y.-N. 1996, ApOpt, 35, 5155
Wang, S., Shen, Y., Jiang, L., et al. 2019, ApJ, 882, 4
Webb, J. K., Flambaum, V. V., Churchill, C. W., Drinkwater, M. J., & Barrow, J. D. 1999, PhRvL, 82, 884
Webb, J. K., King, J. A., Murphy, M. T., et al. 2011, PhRvL, 107, 191101
Webb, J. K., Lee, C.-C., & Milaković, D. 2022, Univ, 8, 266
Webb, J. K., Murphy, M. T., Flambaum, V. V., et al. 2001, PhRvL, 87, 091301
Whitmore, J. B., & Murphy, M. T. 2015, MNRAS, 447, 446
Wills, B. J., Netzer, H., & Wills, D. 1985, ApJ, 288, 94
Yip, C. W., Connolly, A. J., Szalay, A. S., et al. 2004a, AJ, 128, 585
Yip, C. W., Connolly, A. J., Vanden Berk, D. E., et al. 2004b, AJ, 128, 2603
Zhao, G., Zhao, Y.-H., Chu, Y.-Q., Jing, Y.-P., & Deng, L.-C. 2012, RAA, 12, 723